Effect of graphene nanoplatelets on the impact response of a carbon fibre reinforced composite

Elmarakbi, A.[1], Ciardiello, R.[2*], Tridello, A.[2], Innocente, F.[3], Martorana, B.[4], Bertocchi, F.[5], Cristiano, F.[5], Elmarakbi, M.[1], Belingardi, G.[2]

[1]Department of Mechanical and Construction Engineering, Faculty of Engineering and Environment, Northumbria University, Newcastle, NE18ST, United Kingdom

[2]Department of Mechanical and Aerospace Engineering, Politecnico di Torino, Corso duca degli Abruzzi, Turin, 10129, Italy

[3]Delta-Tech S.p.A., località Rifoglieto 60/a - int.1, 55011, Altopascio, LU, Italy

[4]Fiat Research Center, via ex Aeroporto, 80038 Pomigliano d'Arco, Naples, Italy

[5]Nanesa srl, Via Del Gavardello 59/c 52100, Arezzo, AR, Italy

Keywords: Impact behavior; Nano composites; Particle-reinforced composites; Graphene nanoplatelets.

(*) Corresponding author:

Raffaele Ciardiello

Tel.: +39-011-090-6913; fax: +39-011-090-6999.

E-mail: raffaele.ciardiello@polito.it

Abstract

In the present paper, experimental investigations were conducted to assess the effect of nanomodification on the impact behaviours of hybrid composite plates. Graphene nanoplatelets (GNPs) of two different sizes, 5 and 30 µm, were used to modify a composite material made with 64 wt.% of unidirectional fibres and a low-viscosity epoxy resin. The effect of the nanomodification with 30 µm GNPs was also studied on composite plates prepared with a higher viscosity resin. Three laminate thicknesses (4, 8, and 16 layers) were tested with a standard drop dart testing technique. The peak forces as well as the absorbed energy and the fracture surfaces, observed with a Scanning Electron Microscope (SEM), were compared. Experimental results showed that nano-modification with 5 µm particles had a detrimental effect on both the peak forces and the absorbed energy, whereas the addition of 30 µm GNPs increased the absorbed energy, especially for a laminate thickness of 16 layers. Overall, the experimental results demonstrated that the size of graphene nanoparticles has a significant effect on the impact response of composite laminates.

1. Introduction

During the last decade, much effort has been made to provide lightweight designs and materials for the automotive, marine, and aerospace industries. This effort was a direct consequence of the strict regulations regarding the environment, safety, and fuel reduction by the EC [1]. Jambor and Beyer [2] showed that a 7% reduction of vehicle mass can be achieved with structural optimization, while a maximum reduction in the range of 30-50% can be obtained by using advanced high strength steels and aluminium. Larger weight reduction, above 50%, can be obtained only by using composite materials [3, 4], which are characterised by high specific strength and stiffness as well as high resistance to a wide range of environmental conditions and, in some cases, chemical agents [5].

Recently, the nano-modification of composite materials with small weight percentages of particles has been widely investigated to enhance the mechanical and physical properties of the matrices used within composite materials. The use of nano-clays, for example, can lead to an increase of the flexural, compression, and tensile strengths as well as of the moduli, even at high strain rate conditions [6-9]. Carbon nanofibres have been successfully used to improve the delamination resistance, fracture toughness, and flexural strength of glass fibre composites [10-13]. Manero et al. [14] studied the effects that multi-walled carbon nanotubes (MWCNT) had on the energy absorption of a composite made with Kevlar fibres. Comparing the modified panel with the baseline, an 8% increment of the absorbed energy with just 1 wt.% addition of particles, was observed. Kostopoulos et al. [15] studied the effects of the addition of MWCNT in carbon fibre composites. They found that the damage resistance, as well as other mechanical properties of the considered material, can be improved by adding 0.5 wt.% carbon nanotubes. Rahman et al. [16] found that the addition of 1 wt.% oxidized carbon nanofibres improved the impact behaviour of carbon fibre composite laminates.

Furthermore, in the last ten years, the research on nano-modification with the use of graphene nanoparticles has rapidly grown and the study of its effect on the mechanical properties of nano-modified composite materials has been widely researched [17-22]. Graphene particles are characterised by high thermal conductivity (5000 W/mK), high electron mobility, high modulus of elasticity (around 1 TPa), and efficient electrical conductivity [17-22]. One of the most researched areas is that of graphene nanoplatelets (GNPs) due to their ease in production. GNPs are small stacks of exfoliated graphite with a high aspect ratio: although the properties of the single nanoplatelet are exceptionally high, the implementation of graphene in composite materials provides two main challenges. The first is the method used to mix GNPs within the matrix of composite materials, the second the ability to obtain chemical bonds with polymers.

Many authors have studied how to improve the mechanical properties of composites by using graphene particles. Yavari et al. [23] studied the addition of GNP particles in a glass fibre epoxy composite, by spraying graphene particles onto the glass fibres or by infiltrating graphene into the epoxy matrix. They showed that a very low weight fractions of graphene, enhanced nanomodified composite materials were obtained, with notable improvements in their flexural bending fatigue characteristics. Mannov et al. [24] showed that the nano-modification of carbon and glass fibre laminates via the graphene particles had a toughening effect on the composite laminate. Papageorgiou et al. [25] demonstrated that the addition of GNPs (from 5 to 20 wt%) in a polypropylene/glass fibre composite significantly increased the tensile modulus and strength. Pathak et al. [26] carried out experimental tests on hybrid carbon-fibre composites which were reinforced with graphene particles. These reinforced composites were subsequently impregnated with the modified epoxy resin. They showed that the addition of 0.3 wt.% of graphene particles supported the increase of the flexural strength and modulus close to 70%. The impact response of nano-modified composites containing graphene particles was also investigated in the literature [12], with particular attention given to relatively thick plates. Although the investigation of thick composite plates has been widely used, little work has focused on thin hybrid composites.

In the present paper, the impact behaviour of carbon fibre composite plates prepared with a graphene-based modified matrix was investigated. The impact responses of the composite laminates focused on the maximum absorbed energies, the peak loads, and the maximum displacements as established in the ASTM standard D7136 [27]. Two epoxy resins with two different viscosities, 41 and 49 (Pa·s) at 60 °C, were modified by using GNPs. The modified matrixes were used to fabricate carbon fibre composite plates of different thicknesses. The plates were prepared with 0.5, 1.0, and 2.0 mm thicknesses which corresponded to the plates with 4, 8, and 16 layers. Drop dart impact tests were performed to analyse the impact response of the CFRP plates, commonly used in the automotive industry. The used particle concentrations were relatively high due to the viscosity of the used resin. These concentrations, 0.6%, and 0.8%, were the maximum reachable concentrations that allowed for a processable resin for the impregnation of the fibres. Two reasons guided the choice to perform impact tests on these three different thicknesses. The first one was to understand whether there is an influence of the thickness on the impact response of the laminates. To the authors' best knowledge, the effect of the thicknesses of hybrid composites has not yet been studied. The second one was to investigate impact plates with thicknesses that are effectively

adopted in automotive industries. For instance, the thickness of vehicle roofs varies in the range of 1.2-1.7 mm, and the composite plate used to cover the main structure of the bonnet is between 0.6-0.7 mm. Thus, the thicknesses used in this work are compatible with the thicknesses used by the car industry. The main objective of this work is to provide indications regarding the enhancement of the impact response of the composite plates by investigating the number of layers, the particle size and the resin type. SEM analysis was used to study the particle distribution and the fracture surfaces after impact. The effects of the two GNP nano-modifications on impact performance were assessed by comparing the peak forces and the absorbed energy.

2. Materials and methods

The materials and the testing configuration are described in this section. The characteristics of the resin, fibre, and GNPs are reported in Section 2.1. The preparation of the specimens is described in detail in Section 2.2. Finally, the description of the impact test equipment and the test configuration is reported in Section 2.3.

2.1 Materials

Two bisphenol-A based epoxy resins provided by Delta-Tech (Dtech, Italy), commercial name EM120 and EM180, were used for the specimen preparation. EM120 is a relatively low viscosity resin, 41 (Pa·s) at 60°C, with a glass transition temperature of 120 ° C. EM180 is a medium viscosity resin, 49 (Pa·s) at 60°C, with a glass transition temperature of 180 °C. The viscosities of the neat and modified resins (after the addition of GNPs) have been studied by Elmarakbi et al. [28]. These values are reported in Table 1. As shown by [28], the viscosities of the modified resins increase with the addition of the GNPs, and the larger particles increase the viscosity more significantly than the shorter particles.

Table 1: Viscosities of the basic resins and modified ones [28]

Sample	Viscosity (Pa·s) at 60°C	Minimum viscosity (Pa·s) (temperature)
EM120	41	0.7 (107 °C)
EM120-GNaN_0.8%	77	1.1 (105 °C)
EM120-GAvA_0.8%	50	1.1 (106 °C)
EM180	49	1.1 (114 °C)
EM120-GNaN_0.6%	68	2.0 (115 °C)

All the specimens were produced by using unidirectional carbon fibres, 150-UTS50 (F13) UD, provided by Tenax Europe (Germany). The unidirectional carbon fibres are (UD) tape 600 mm wide, having a fibre areal weight of 150 $\frac{g}{m^2}$. The resin content of the composite plates is 36 wt.%. The UD prepregs were used to prepare cross plays with the following configurations $[+45\ -45]_2$, $[+45\ -45]_4$, and $[+45\ -45]_8$. Two different GNPs were chosen in order to verify the effect of particle size on the

mechanical performance of the tested composite materials, GNaN and GAvA. The GNaN particles have a particle size of 30 µm while GAvA particles have an average size of 5 µm. The GNaN particles provided by NANESA S.r.l. (Arezzo, Italy) are produced using a non-oxidative process via liquid-phase exfoliation (LPE) of graphite. The average lateral size is 30 µm (D50=25 µm) and the average flake thickness is 9 nm (about 40 layers). C:O (carbon to oxygen) atomic ratio as measured by X-ray photoelectron spectroscopy (XPS) is 44:1. GNaN has a bulk density of ~0.02 g/cm^3. The GAvA particles provided by Avanzare Innovacion Tecnologica (La Rioja, Spain) are also produced using a non-oxidative process via liquid-phase exfoliation (LPE) of graphite. The average lateral size is 5 µm (D50=5 µm) and the average flake thickness is 3 nm (about 8-9 layers). C:O (carbon to oxygen) atomic ratio as measured by X-ray photoelectron spectroscopy (XPS) is 100:1. GAvA has a bulk density of ~0.02 g/cm^3. No treatments were carried out on the particles.

2.2 Specimens preparation

As a preliminary analysis, three different methods were considered for the dispersion of the GNP particles within the epoxy matrix, namely, three-roll mill, high shear mixing, and sonication. The high shear mixing method was identified as the most suitable technique to mix the resin and the graphene by considering the obtained dispersion of GNP particles. This mixing method consists of two phases. The particles are mixed with a shaft dispersion system that uses Cowles blades at 2000 rpm for 60 min in the first phase. In the second phase, the nanoparticles were distributed and homogenized within EM120 resin (weight percent of 0.8%) and EM180 resin (weight percent of 0.6%) using a Silverson high shear mixing system at 3000 rpm for 30 min. The different nanoparticle weight percentages depend on the viscosity of the resins, the reported values correspond to the maximum reachable concentration that allows for a processable resin. After the mixing phases, the nanomodified resins were used to impregnate the carbon fibres and to obtain prepreg layers (100x100 mm) with the unidirectional carbon fibres and with a thickness equal to 0.125 mm. They were prepared with neat and the modified resins by Delta-Tech. The layers were then stacked by using the hand lay-up process and cured in a mechanical press by applying a pressure of 0.3 MPa. In particular, EM120-based resins were cured under the press for 90 min at 120 °C, whereas EM180-based resins were cured for 90 min at 135 °C under press and post cured in the oven for 120 min at 180 °C. In both cases, the heating rate was 1 °C/min. Three different laminate thicknesses were manufactured: 0.5±0.05 mm (4 layers), 1.0±0.05 mm (8 layers), and 2.0±0.05 mm (16 layers). Table 2 reports all the materials tested in this work. Three test replications were performed for each investigated composition.

Table 2: Summary of the tested specimens

		Number of layers	Stacking sequence
EM120	Neat resin	4; 8; 16	$[+45\ -45]_2$; $[+45\ -45]_4$; $[+45\ -45]_8$
	EM120+GNP Avanzare	4; 8; 16	
	EM120+GNP Nanesa	4; 8; 16	
EM180	Neat resin	4; 8; 16	
	EM180+GNP Nanesa	4; 8; 16	

The impregnation of the fibres with the composite matrix was verified by using a Scanning Electron Microscope (Model ZEISS Supra 40). In order to obtain the best resolution, secondary electron emission signals were used with an accelerating voltage of 1.4 kV. The specimens were properly coated with gold to have better images [29]. The results of the Scanning Electron Microscope (SEM) are discussed in Section 3.3.

2.3 Impact equipment

Impact tests were carried out using a free-fall drop dart testing machine (CEAST 9350 FRACTOVIS PLUS) equipped with a 20 mm hemispherical impactor tup. This testing machine is instrumented with a piezoelectric load cell (203B by PCB Piezotronics, Depew, United States), located just behind the impactor tup, to measure the impact force history. The tests were carried out at an impact speed of 5.7 m/s. It was selected after some preliminary quasi-static tests on the specimens in order to induce the perforation in all the investigated plates. An impact mass of 22.3 kg was used in order to have a final impact energy of 362 J. The level of 362 J was chosen after a preliminary quasi-static test activity conducted on the specimens BL16 and AL16. They presented values of the average maximum absorbed energies of 181 J and 161 J respectively. For the dynamic tests, the maximum value of the absorbed energy obtained in the quasi-static tests was doubled to obtain the perforation.

The impact speed was measured using a magnetic encoder for each impact test. The encoder measures the speed of the impactor just before it comes into contact with the specimen to accurately evaluate the impact energy. The speed signal was also used as a trigger to start the acquisition of the load signal, to reduce the amount of data acquired and stored. The tested specimens were fixed by a mechanical clamping system which ensures uniform pressure all over the clamping area, as shown in Figure 1.

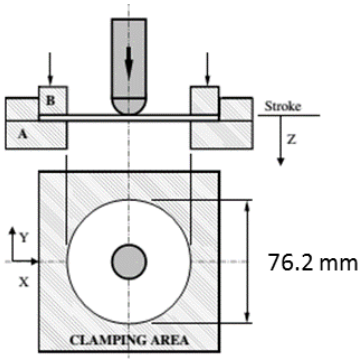

Figure 1: Clamping system for the impact tests. In shadowed grey, the clamped area [29].

The load signal was acquired with a sample rate of 1 MHz. According to the procedure described in [30-32] and by considering the energy balance equation during the impact, the displacement-time curve was obtained. This was done by integrating twice the acceleration time history, calculated from the acquired load signal, with respect to time, taking into account the initial value of the velocity. The absorbed energy was finally obtained through an additional integration of the load with respect to the displacement.

3.Experimental results

The experimental results are analysed in this section. The results of the analysis carried out by using the SEM are reported in Section 3.1. Section 3.2 reports the results of the impact tests and the analysis of the effect of the nano-modification on the impact response. Finally, the fracture surfaces are analysed in Section 3.3. In the following, the material fabricated with the resin EM120 are referred to with the letter A, whereas the materials fabricated with the resin EM180 are referred to with the letter B. Furthermore, the letter L is added to the nomenclature of the material that embeds larger GNPs (GNaN), whereas the letter S is used for the materials that embed shorter GNPs (AVA). The neat materials, which are the materials prepared with the unmodified resins and the carbon fibres, are named NA for the resin EM120 and NB for the resin EM180. The nomenclature is finally completed by the use of the number of layers, which are 4, 8, and 16. For example, AL4 refers to the four-layer composites obtained with the resin EM120 impregnated with larger GNPs (GNaN).

3.1 Scanning electron microscope analysis

Representative images of the SEM analysis carried out on the modified matrixes A and B are shown in Figures 2, 3, and 4. The SEM analysis was carried out on squared samples with a lateral size of 30 mm. This analysis investigated the distribution of the particles. The samples were analysed in different points to identify possible nonuniform particle distributions. Due to the large area analysed, Figures 2, 3, and 4 can be assumed as representative of the nanoplatelet dispersion within the epoxy matrixes. Figure 2a displays a representative image of the dispersion of 30 µm GNPs within the resin A. The presence of the particles looks uniform and no agglomerates are present. Figures 2b, c and d show higher magnification of the particle dispersion, the particles look well

distributed without the presence of agglomerates. Figures 3a, b, c, and d show the distribution of the 5 µm particles within the resin A at different magnifications. Figure 3a shows that the distribution of the GNPs is quite uniform except for some darker areas, highlighted with red ellipses, in which a lack of particles is observed. Figure 3b displays one of the areas where the particles were not uniformly distributed. In particular, a small agglomerate in which some particles are in contact is visible for the AS matrix. This can be correlated to reduced impact properties of these composites, that is discussed in Section 3.2. Figures 3c and d show single particles well embedded in the epoxy matrix. The size of the particle is close to the average value of 5 µm reported by the datasheet. Figures 4a, b, c, and d show the distribution of 30 µm particles embedded within the matrix B at different magnifications. Figure 4a illustrates that the particle distribution is quite uniform. Although the particles are close, no agglomerates were found and the particles do not touch each other as shown Figures 4b, c, and d at higher magnifications.

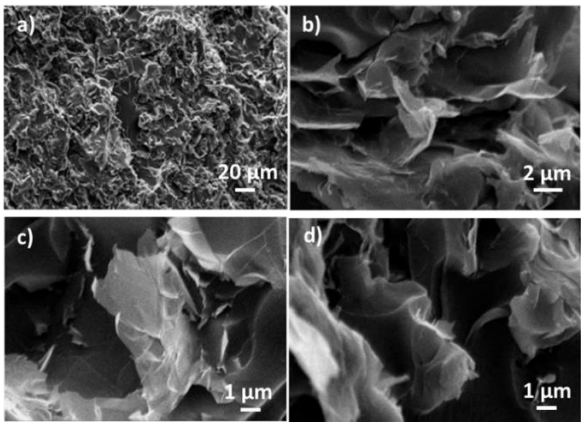

Figure 2: Dispersion of the 30 µm particles in the resin A at different magnifications: a) 1 kX; b) 12 kX; c) 16 kX; d) 20 kX

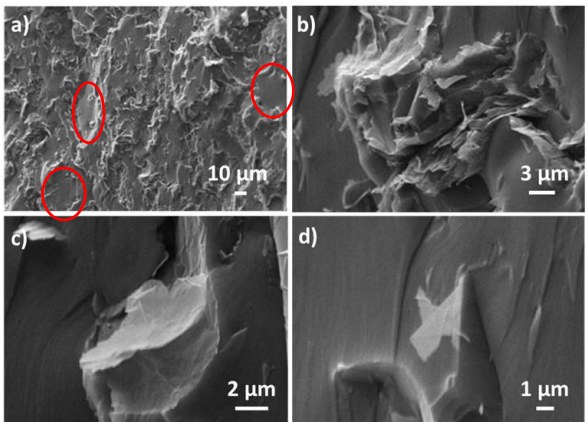

Figure 3: Dispersion of the 5 µm particles in the resin A at different magnifications: a) 1 kX; b) 8 kX; c) 15 kX; d) 20 kX

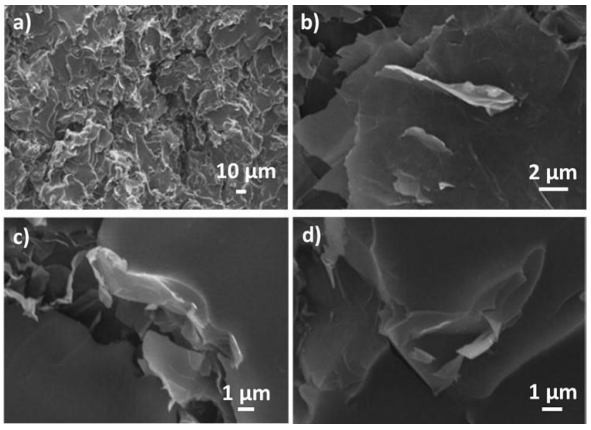

Figure 4: Dispersion of the 30 µm particles in the resin B at different magnifications: a) 1 kX; b) 15 kX; c) 16 kX; d) 20 kX

The SEM analysis showed also that the fibres and the nanoplatelets were well impregnated by the resins, as visible in Figures 5a and b. Figures 5a and b show the presence of the resin over the fibres and this led to good interaction between matrix and fibres. The SEM image at the bottom, Figure 5c, shows the edge of a GNP, marked with a white arrow, which is fully integrated into the resin,

showcasing the strong interaction between the GNP and the resin. Figures 5a and 11b show that the fibres are still well impregnated by the matrix also after the impacts.

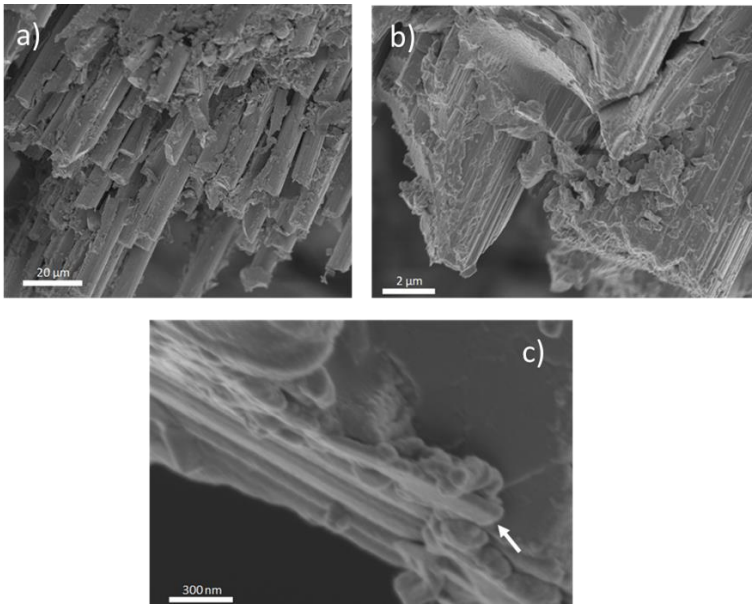

Figure 5: Representative SEM images of the composite plates at different magnifications in the fractured area: a) 2.5 kX; b) 22 kX; c) 190 kX

3.2 Impact response

The representative force-displacement curves relative to the specimens prepared with resin A and the larger GNPs are presented in Figure 6. The figure confirms that there is an expected increase in the stiffness of the plates by increasing the number of layers.

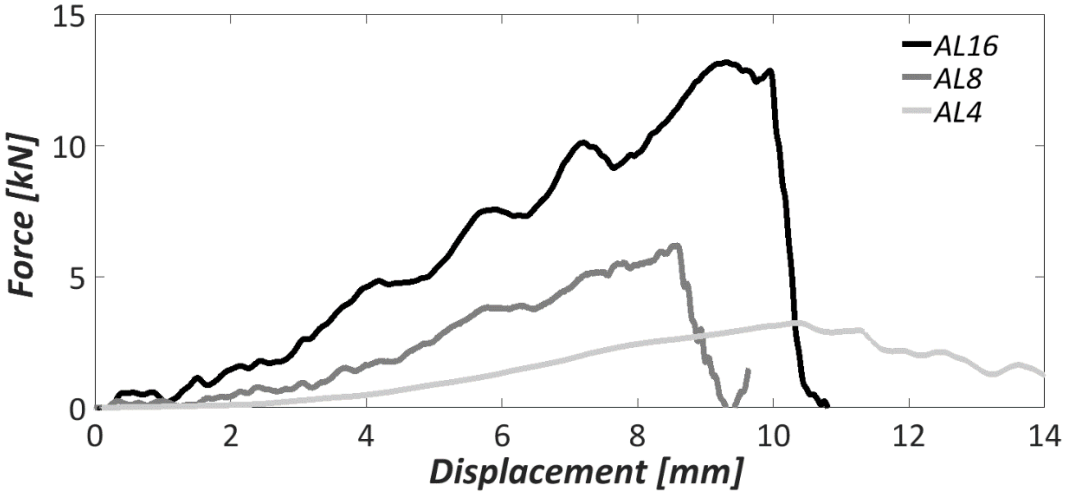

Figure 6: Representative force-displacement curves of the modified resin EM120

The energy – displacement curves which are used for comparing the impact response and consequently for discussing the effects of the considered factors are shown in Figure 7. In particular,

the energy – displacement curves for the neat, the composite plates nanomodified with small, and large GNPs are compared in Figure 7a (4 layers), in Figure 7b (8 layers) and Figure 7c (16 layers). All the tests performed resulted in the final perforation of the specimens, as targeted when the impact test parameters were selected. As can be seen in Figure 7, the energy absorbed at the perforation of the plates after the nano-modification with the shorter particles is always lower than the absorbed energy of the neat and the nanomodified plates with larger particles, as well as the maximum reached displacement. It can also be noted that the absorbed energies at the perforation of the composite plates that embed larger GNPs are larger than those of the neat plate for all three specimen thicknesses considered.

Moreover, Figures 7a and 7b provide evidence that the values of the absorbed energies at the perforation of the composite plate prepared with 4 and 8 layers are very close. This is mainly due to the different trends of the force-displacement curves after the peak load seen in Figure 6. The curve for the composite laminate prepared with 8 layers shows a lower value of the displacement at the perforation and a rapid decrease of the load after the maximum peak (comparable with that of the AL16 composite laminate). On the other hand, the curve for the composite laminate prepared with 4 layers presents a larger value of the displacement at the perforation (comparable with that of the AL16 composite laminate) and a subsequent smoother decrease. This leads to comparable values of the absorbed energy despite the larger value of the maximum load reached by the composite laminate prepared with 8 layers.

a)

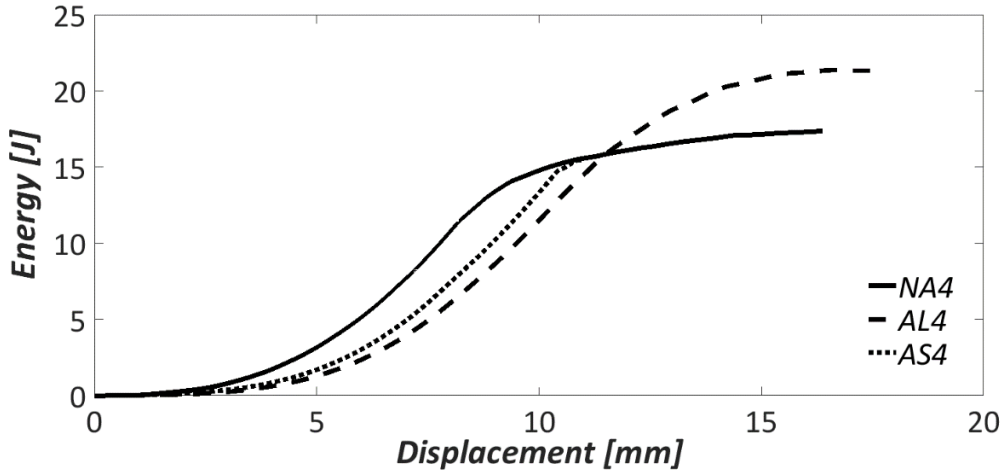

b)

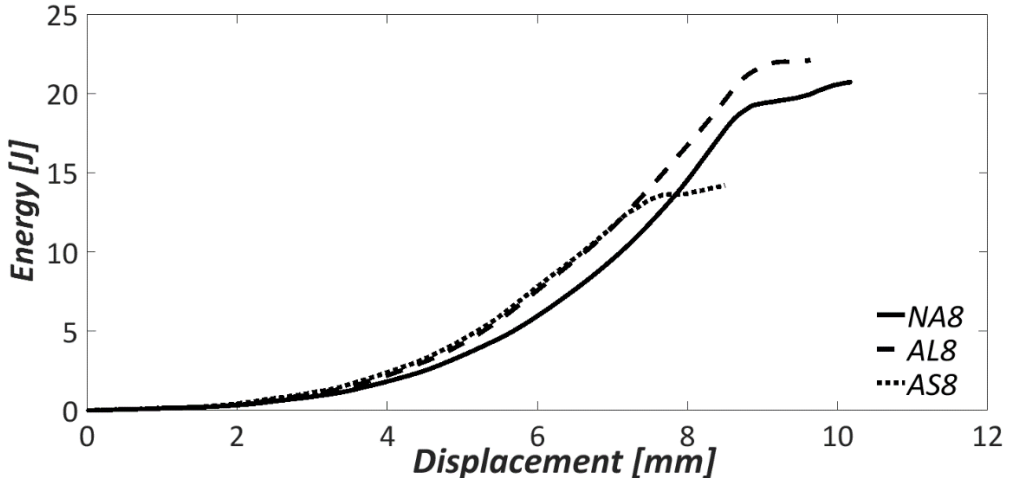

c)

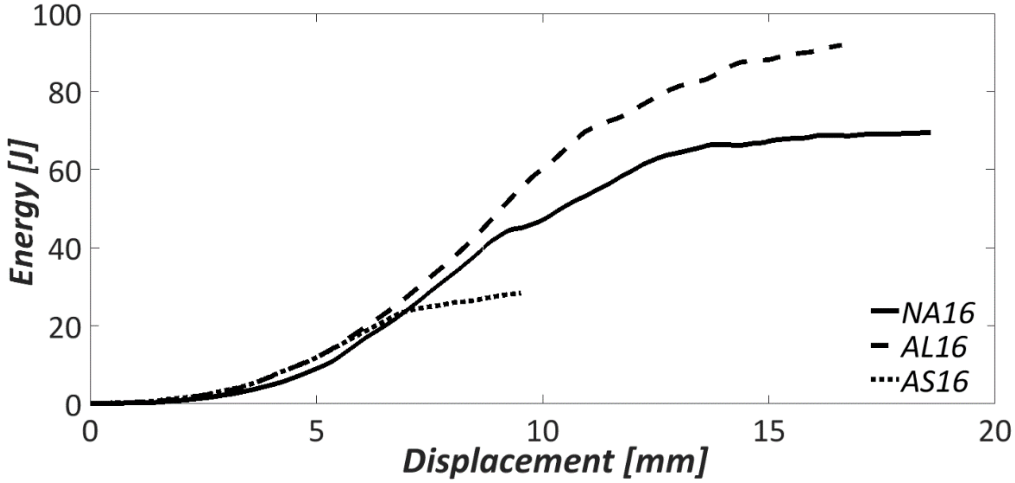

Figure 7: Comparison of the energy – displacement curves: a) 4 layers; b) 8 layers; c) 16 layers.

The peak forces and the absorbed energies for all the neat composite plates tested and the plates modified with larger and shorter particles are reported in Figure 8. The standard deviations of the parameters investigated are also shown in the bar plot. As previously highlighted, the absorbed energy of AS specimens is shorter for the three thicknesses investigated (4, 8, and 16 layers). Although there is no significant difference in the peak force for the composite plates made of 4 layers, the absorbed energy of AL4 is higher, as reported in Figure 7a. On the other hand, the average peak force experimentally assessed on NA8 plates is larger than the peak force measured on AL8

plates but by contrast, the absorbed energy at the perforation of AL is higher. The peak force and the absorbed energy for the AS8 are smaller than the corresponding values measured on NA8 and AL8.

The analysis of the peak loads of the composite plates which are made of 16 layers shows that AL16 presents the highest peak load (10% higher than the NA16), while the peak force of AS16 is the lowest. The same results have been found for the absorbed energy at perforation. The values of the absorbed energy for AL16 is 10% higher than the neat plate, while the absorbed energy for AS16 is the lowest (60% lower than NA16).

The experimental results show that the nano-modification of composites containing the shorter graphene particles had a negative influence on impact response. The effect of the GNP size particles on the impact response of the composite plates has been investigated by Wang et al. [33] and Ervina et al. [34]. They found that the particle size significantly affects the mechanical properties of nano modified plates. Wang et al. [33] studied the effect of two nanoparticles with different sizes. They found that the quasi-static performance can be enhanced by the use of larger sized GNP particles with respect to the neat condition. This effect was evident for both Young's and the flexural moduli, which are both involved in the damage mechanisms when impact loads are applied. Wang et al. [33] showed that the dispersion of the larger particles was more uniform compared to the shorter particles. The experimental results obtained in the present work confirm that the results obtained in [33], which were quasi-static tests, are also valid for impact tests. Moreover, Ervina et al. [34] reported that when shorter nanoparticles are not properly and uniformly dispersed within the matrix, they are not able to transfer the loads between the matrix and the fibre. On the other hand, the particles may act as defects, leading to a reduction of the impact response after the nanomodification. Wang et al. [35], in a different work, studied the size effect of two different graphene nanoplatelets on the mechanical behaviour of glass fibre/epoxy composites. The morphology analyses carried out by these authors showed that larger GNPs were present between the adjacent glass fabrics, and were not able to penetrate into the interstices of fibres due to their large lateral dimension. By contrast, shorter GNPs penetrated inside the intervals of fibres but with visible agglomerates due to their small size and large specific surface area. The mechanical studies presented in their work showed that the flexural modulus and storage modulus of the glass fibre/epoxy composite decreased for the composite plates prepared with shorter particles due to their presence between the fibres. The presence of the GNP particles between the fibres was also reported by Elmarakbi et al. [28] that used the carbon fibres and particles (GNaN and GAvA) used in the present work with a slightly different resin. The work reported that the shorter particles (AVA) penetrated between the particles as reported. By contrast, the composite plate prepared with larger GNPs (GNaN) do not present the same behaviour. As showed by Wang et al. [35], this behaviour in addition to the presence of some agglomerates, which has been reported in Figure 3, led to a detrimental effect of the mechanical properties. The results obtained in the present study confirm the effects outlined above.

As a conclusion, the enhanced impact response of nano modified composites with larger particles is mainly due to their capability of obstructing and deflecting the micro-cracks which initiates during the impact, thus absorbing a larger amount of energy. This beneficial mechanism is not present for

the nanomodified composite with shorter nanoparticles, where the GNPs act as defects due to their non-uniform dispersion, thus inducing a reduction of their impact properties.

However, the improvement of impact response due to the GNP nano-modification is only evident for the plates with the largest thickness (16 layers), as shown in Figures 7 and 8. The nano-modification with larger graphene particles led to an average increment of the peak force as well as the absorbed energy of about 10% compared to the neat case for the largest plates. This can be due to the different damage mechanisms that are involved in thin and thick laminates. During an impact, different damage mechanisms are involved. For example, delamination starts in the impact region and grows wider through the thickness, and the nanoparticles placed in the bottom layers are responsible for the enhancement of the impact response with respect to the neat condition [36]. For this reason, for plates with small thicknesses, the strengthening mechanism resulting from to the nanomodification is not effective due to the small number of layers. This justifies why the effect of the nanomodification is evident only for the plate with the largest thickness or, better, with the largest number of layers.

Moreover, according to [37], for thin laminates, the membrane behaviour dominates and is the main cause for their initial damage. In this case, the stiffness variation is correlated to differences in thickness (between the neat and the nanomodified plate). On the other hand, for thick laminates, a flexural behaviour dominates and is the main cause of damage. In this case, the stiffness variation among the laminates is supposed to be correlated to the thickness at the third power. Therefore, for plates with 4 and 8 layers, there could be a possible influence on the impact response and on the stiffness of the plates, depending on the thickness difference between the neat and the nanomodified plates. Specific thickness measurements were performed and this difference proved to be negligible. By contrast, for the plate with the largest thickness for which flexural damage can be present, even small differences in thicknesses due to the nanomodification can have a non-negligible effect. This can also be the reason for the larger scatter found experimentally for the 16-layer plates, by considering, for example, the absorbed energy.

Moreover, the experimental results show that the effect of the nanomodification is more relevant for the absorbed energy than for the peak force. This result can be explained by considering the damage mechanism. According to [38], the presence of nanoplatelets mainly induces higher dissipative mechanisms, that justify the large increment of the absorbed energy and the limited increment of the peak force.

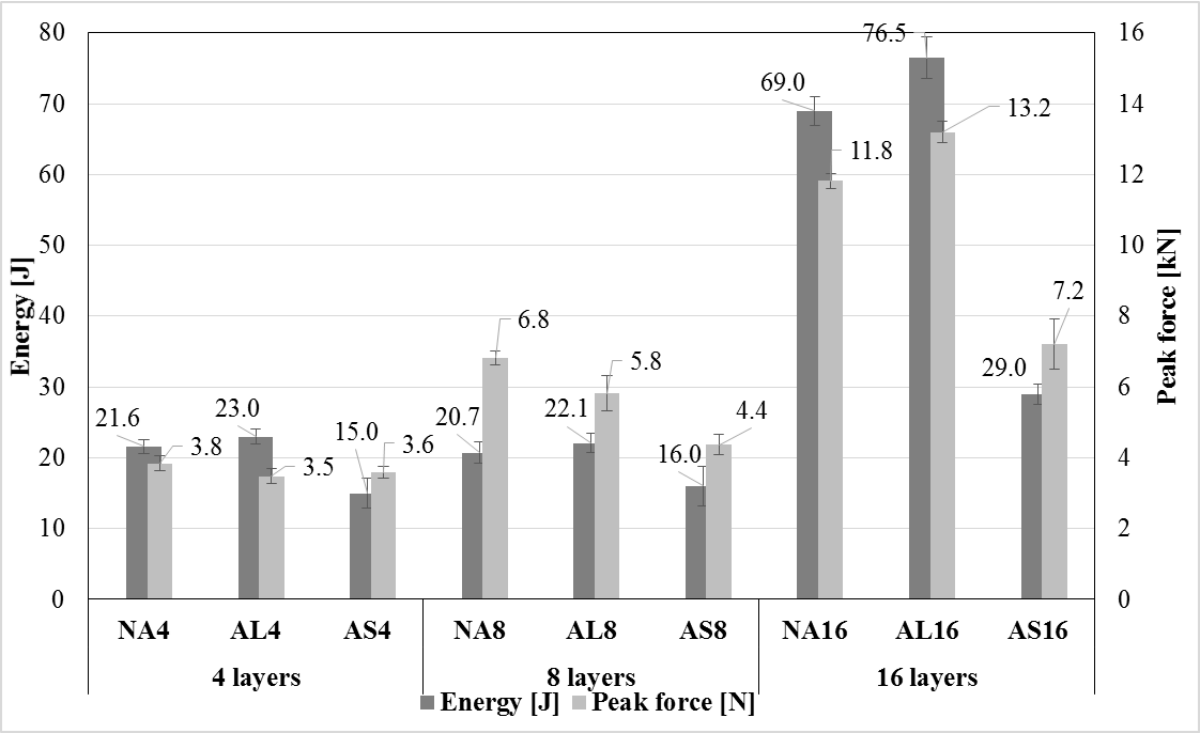

Figure 8: Bar plot of the absorbed energy and the peak force of the resin EM120

Representative force-displacement curves for the resin B modified with the larger GNPs are shown in Figure 9. The expected increment of plate stiffness in comparison with the number of layers is shown in Figure 9. Furthermore, these curves are slightly different compared to those prepared with resin A. In the authors' opinion, this could be due to the different properties of the resin, as confirmed by the analysis of the fracture surfaces (Section 3.2)., Observations of the curve trends reveal that the main difference is due to the change of the force signal after the peak load in the BL16 composite, which does not decrease as rapidly as with AL16, AL8, and BL8. This can be due to the friction between the intact fibres and the dart tup that prevents a rapid decrease of the load.

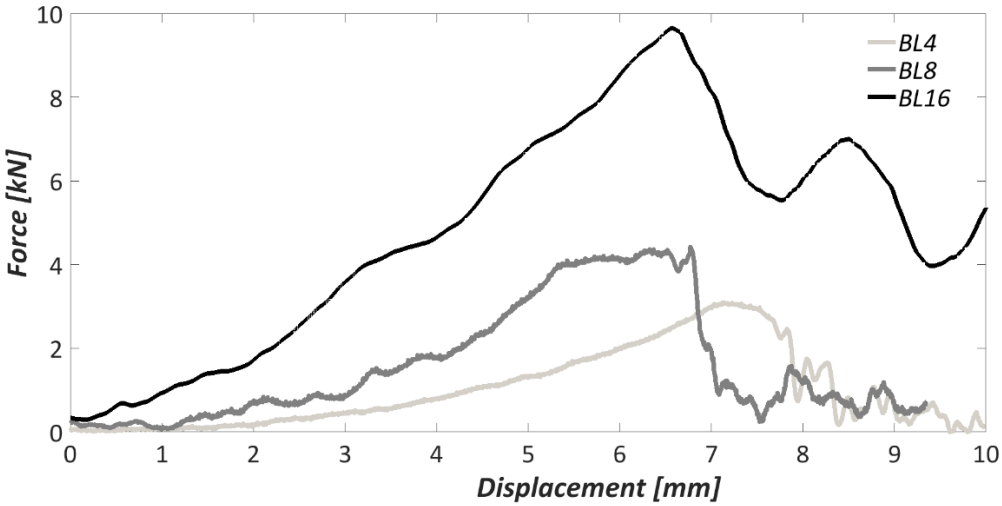

Figure 9: Representative force-displacement curves of the modified resin EM180

The comparison of the energy – displacement curves for the neat composite plates and those nanomodified with the large GNPs, for the three thicknesses, are displayed in Figure 10. Figure 10 illustrates that the absorbed energy for the composite plates modified with larger particles is slightly higher than the neat cases for the composite plates prepared with 4 and 8 layers. On the other hand, the absorbed energy for the BL16 is significantly larger. Furthermore, while the maximum reached displacements of the NB and BL specimens are almost equal for 4 and 8 layers, the value of the displacement of BL16 is much larger compared to NB16.

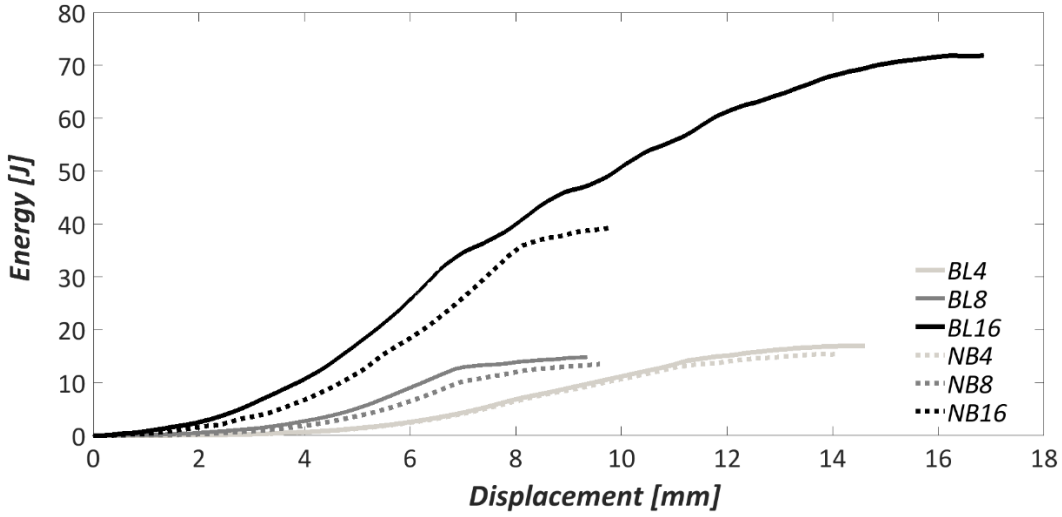

Figure 10: Comparison of the energy – displacement curves for the modified resin EM180

The average values of the absorbed energies occurring at perforation and the peak forces of resin B alongside with the corresponding standard deviations are reported in the bar plot in Figure 11. The values of the absorbed energies and the peak forces change with the same trend as for resin A, the values for the 4 and 8 layer composites do not change significantly. The nano-modification leads to an increase of the peak load (8% higher compared to the neat plates) only for the plates with 16 layers as for resin A. On the other hand, the absorbed energy for BL16 is significantly larger, about 80%, compared to the neat plates. The values of the peak forces and the absorbed energy for resin B (16 layers) are significantly higher when compared.

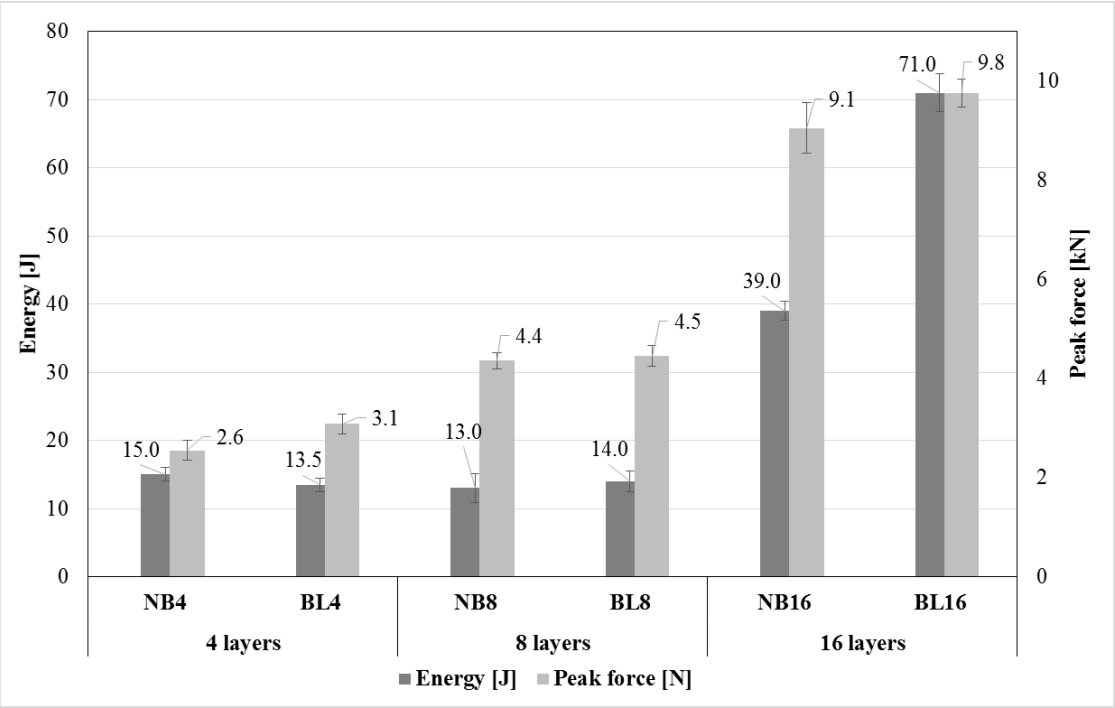

Figure 11: Bar plot of the absorbed energy and the peak force for the resin EM180

The exponential trends extrapolated by the average values of the peak loads (Figure 12a) and the absorbed energies (Figure 12b) are presented in Figure 12. The values of the peak loads and the absorbed energies assessed through the tests performed on resin A are higher compared to those obtained with tests performed on resin B. Furthermore, they show that the 4 and 8 layer plates had extremely similar values for peak loads and energy, as shown in Figure 8 and 11, which includes the standard deviation. On the other hand, the values of the peak load and the energies for the composite plates prepared with 16 layers are higher for the composite plates that embed larger particles. To the best of the author's knowledge, no existing experimental results show the effect of nano-modification on the impact response of plates with a thickness smaller than 2.4 mm, to compare the results obtained through tests on plates with 4 and 8 layers. The studies [9], [15], [16], and [39] reported impact tests conducted on composite plates with thicknesses between 2.4 and 3.1 mm. The increase of absorbed energy by the addition of GNPs was also found in [12], where glass-reinforced multilayer composites modified with GNPs were studied. A slight increase of the absorbed energy was also found in [9] and [15] where the modification of the matrix was performed using nano-clays and multi-walled carbon nanotubes, respectively. Higher absorbed energies were obtained in [39] by using carbon nano-fibres. However, the maximum increase of the absorbed energy was 52%, which is lower than the maximum increase obtained in the present work.

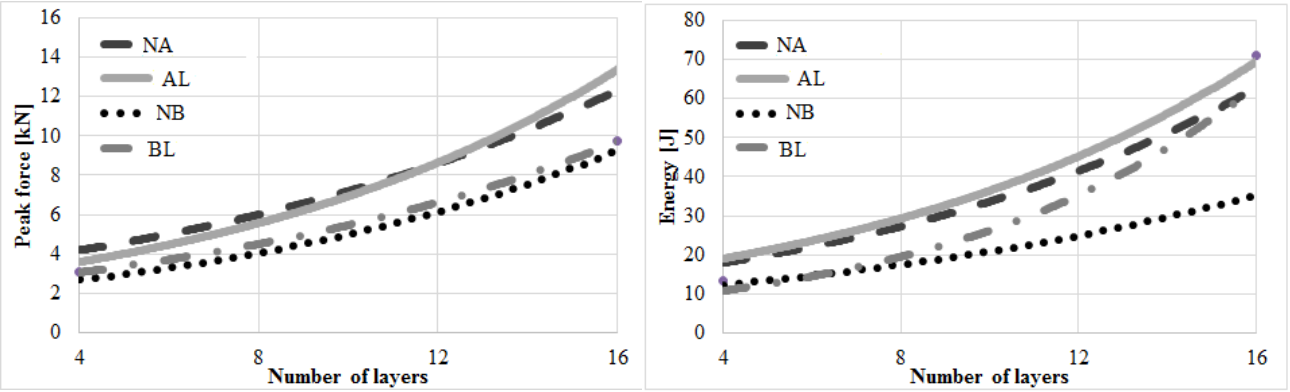

a) b)

Figure 12: Exponential distribution of the peak load (a) and the energy (b) neat resin and the modified ones

3.3 Fracture surfaces

Representative fracture surfaces of the composite laminates prepared with resin A for 4, 8, and 16 layers are shown in Figure 13. The three rows illustrated in Figure 13 show the fractured plates of the neat resin, the modified resin with larger particles, and the modified resin with the shorter particles. The fracture surfaces can be separated into two typical breaks. The fracture surfaces of NA8, AL4, AL8, AL16, and AS8 present clear fracture surfaces that are limited to the area related to the impact tup. On the other hand, the fracture surfaces of NA4, NA16, AS4, and AS16 present fracture surfaces which also involve some fibres close to the area of the impact tup. All the surfaces modified with larger particles present a cleaner break. Although two different typical fractures are identified, there is not a direct correlation between the fracture surfaces, the maximum peak loads and absorbed energies. In fact, the fracture of the specimen NA8, AL8, and AS8 look very similar but they led to different impact responses in terms of peak loads (6.8, 5.8, and 4.4 kN) and impact absorbed energies (20.7, 22.1 and 16.0 J). For this reason, the enhancement or the detrimental effects of the impact behaviour is not directly linked to the morphology of the fracture surfaces but need to be found in the dispersion of the particles or the particles size and their capacity of obstructing and deflecting the cracks formed during the impact, as has been discussed in detail in Section 3.1. All the fracture surfaces present a diameter of 20 mm that is the diameter of the impact tup.

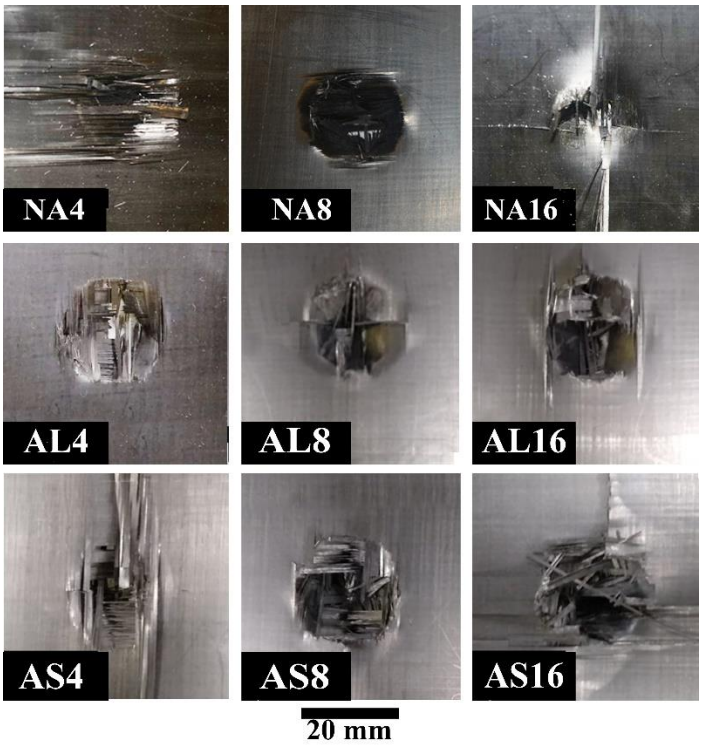

Figure 13: Fracture surfaces of the composite plates prepared with resin A

The fracture surfaces of the composite laminates prepared with resin B are presented in Figure 14. All the fracture surfaces are very similar to the fracture surfaces of the plates shown in Figure 12 for the three cases considered. Also in this case, the differences in the mechanical properties are not directly linked to the fracture surface but have to be found in the dispersion of the particles that, as shown in Section 3.1, are uniform and led to improved mechanical properties for the composite plate BL16. These fracture surfaces display some intact fibres that probably led to an increment of the load after the perforation in place of the typical drastic reduction to 0 of the force signals. All the fracture surfaces also here present a diameter of 20 mm, that is the diameter of the impact tup.

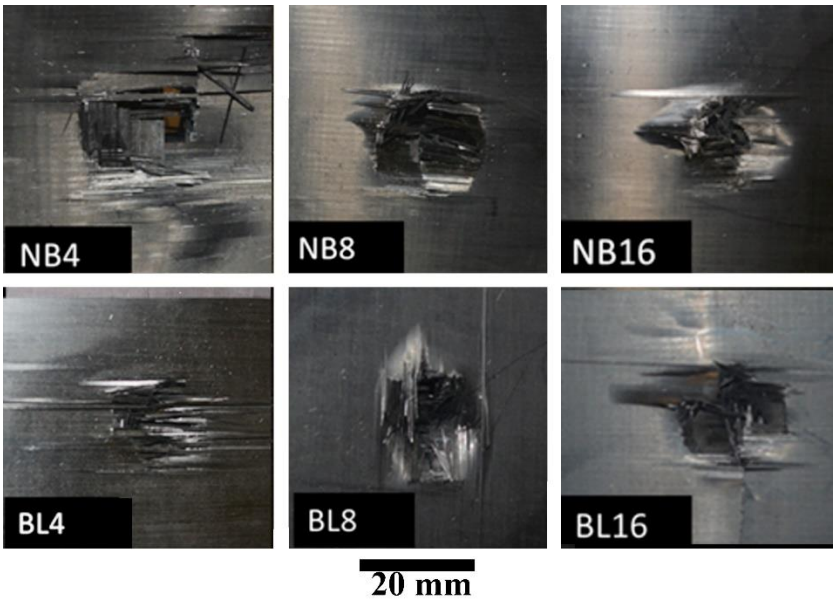

Figure 14: Fracture surfaces of the composite plates prepared with resin B

Conclusions

The impact behaviour of hybrid composite laminates made with GNPs and unidirectional carbon fibres were investigated by using drop dart impact tests. Two GNPs were used for specimen production: 5 µm GNPs (GAvA) and 30 µm GNPs (GNaN), supplied by two different manufacturers and they were used to modify a low viscosity resin, EM120. Furthermore, the second set of specimens was obtained by embedding GNaN particles within a resin with a higher viscosity, namely EM180. The main results of this work are summarized as follows:

- The addition of 5 µm particles to resin EM120 had a detrimental effect on the composite plates under impact for all the adopted configurations (4, 8, and 16 layers) with respect to the composite plate without nanoparticles. The worst result regard the 16 layers composite laminates, which showed a reduction of the absorbed energy (58%) as well as a reduction of the peak force (38%).
- The addition of 30 µm particles to resin EM120 allowed an increase of the absorbed energies in all the composite plates. The effect of the nano-modification is more evident for the thickest specimens (16 layers), with a 10% increment of both the absorbed energy and peak load compared to the neat composite material (not nanomodified).
- The addition of 30 µm particles to resin EM180 shows that the values of the energies and the peak forces change with a trend similar to resin A. The values for the 4- and 8-layer plates do not change significantly except for the values of the peak load of BL4, that is 20% higher. The nano-modification leads to a very large increase in the absorbed energy for BL16 compared to the neat plates (around 80%).
- Visual observation of the fractured specimens shows that the fracture surfaces can be separated into two different types. However, the enhancement or the detrimental effects

of the mechanical properties are not directly linked to the macroscopical evidence presented in the fracture surfaces. By contrast, they need to be found in the nature of the hybrid structure of the composite plates that led to detrimental mechanical properties for composite plates prepared with shorter particles, due to the non-uniform dispersion of the GNPs.

- The SEM analysis revealed that the fibres and nanoplatelets were still well impregnated by the resins. The SEM analysis showed the fibres that were still impregnated although they were pulled out from the matrix. Furthermore, the images of the particle dispersion show that the larger particles are uniformly dispersed in the epoxy matrix, whereas the shorter particles were not opportunely dispersed.

Overall, this work demonstrates that the size of GNPs significantly affected the impact response of the investigated composite plates. Larger GNPs enhanced the impact response of composite materials, while shorter GNPs had a detrimental effect on the impact behaviour of composite plates. Furthermore, nano-modification did not affect thin composite plates with 0.5 and 1.0 mm thickness (i.e., the difference is only related to the experimental scatter), whereas it is evident for the 16-layer composite plates, where there was more than a 10% difference. Therefore, it can be concluded that the use of large GNPs on composite plates with at least 16-layer plate, which are the most commonly used, equates to a relevant enhancement of the impact response.

Acknowledgment

The research leading to these results has received funding from the European Union Seventh Framework Programme under grant agreement No. 604391 and Horizon 2020 Programme under grant agreement No. 696656 Graphene Flagship

References

[1] G. Belingardi, E. Koricho, B. Martorana, Design optimization and Implementation of composite and recyclable thermoplastic materials for automotive bumper, Int. J. Automot. Compos. 1(1) (2014) 16-30.

[2] A. Jambor, M. Beyer, New cars-new materials, Mater. Des. 18(4/6) (1997) 203-209.

[3] Y. Li, Z. Lin, A. Jiang, G. Chen, Experimental study of glass-fiber mat thermoplastic material impact properties and lightweight automobile body analysis, Mater. Des. 25 (2004) 579-85.

[4] G. Belingardi, J. Obradovic, Recent development in car body lightweight design - a contribution toward greener environment, Mob. & Vehic. Mec. 38(4) (2012) 9-23.

[5] A. Ashor, Wood–plastic composites as promising green-composites for automotive industries, Bioresour. Technol. 99(11) (2008) 4661-4667.

[6] J. Bibin, N.C.P. Reghunadhan, K.N. Ninan, Effect of nanoclay on the mechanical, dynamic mechanical and thermal properties of cyanate ester syntactic foams, Mater. Sci. Eng. A. 527(21-22) (2010) 5435–43.

[7] R. Maharsia, N. Gupta, H.D. Jerro, Investigation of flexural strength properties of rubber and nanoclay reinforced hybrid syntactic foams, Mater. Sci. Eng. A. 417(1-2) (2006) 249–58.

[8] S. Peter, E. Woldesenbet, Nanoclay syntactic foam composites—high strain rate properties, Mater. Sci. Eng. A. 494(1–2) (2008) 179–87.

[9] E.G. Koricho, O. Karpenko, A. Khomenko, M. Haq, G.L. Cloud, l. Udpa, Evaluation of progressive damage of nano-modified composite laminates under repeated impacts, Proc. SPIE Int. Soc. Opt. Eng. 98 (2016) 1-13.

[10] J.N. Baucom, M.A. Zikry, A.M. Rajendran, Low-velocity impact damage accumulation in woven S2-glass composite systems, Compos. Sci. Technol. 66(10) (2006) 1229-1238.

[11] R. Sadeghian, S. Gangireddy, B. Minaaie, K. Hsiao, Manufacturing carbon nanofibers toughened polyester/glass fiber composites using vacuum assisted resin transfer molding for enhancing the mode-1 delamination resistance, Compos. Part. A. Appl. S. 37 (2006) 1787–1795.

[12] N.T. Kamar, M.M. Hossain, A. Khomenko, M. Haq, L.T. Drzal, A. Loos, Interlaminar reinforcement of glass fiber/epoxy composites with graphene nanoplatelets, Compos. Part A Appl. S. 70 (2015) 82–92.

[13] R. Ciardiello, L.T. Drzal, G. Belingardi, Effects of carbon black and graphene nano-platelet fillers on the mechanical properties of syntactic foam, Compos. Struct. 178 (2017) 9–19.

[14] M.A. Albert, J. Gibson, G. Freihofer, J. Gou, S. Raghavan, Evaluating the effect of nano-particle additives in Kevlar® 29 impact resistant composites, Compos. Sci. Technol. 116 (2015) 41-49.

[15] V. Kostopoulos, A. Baltopoulos, P. Karapappas, A. Vavouliotis, A. Paipetis, Impact and after-impact properties of carbon fibre reinforced composites enhanced with multi-wall carbon nanotubes, Compos. Sci. Technol. 70 (2010) 553-563.

[16] M. Rahman M. Hosur, K.T. Hsiao, L. Wallace, S. Jeelani. Low velocity impact properties of carbon nanofibers integrated carbon fiber/epoxy hybrid composites manufactured by OOA–VBO process, Compos. Struct. 120 (2015) 32–40.

[17] D.G. Papageorgiou, I.A. Kinloch, R.J. Young, Mechanical properties of graphene and graphene-based nanocomposites, Prog. Mat. Sci. 90 (2017) 75-127.

[18] K.S. Novoselov, A.K. Geim, S.V. Morozov, D. Jiang, Y. Zhang, S.V. Dubonos, Electric field effect in atomically thin carbon films, Sci. 306 (2004) 666–669.

[19] A.A. Balandin, S. Ghosh, W. Bao, I. Calizo, D. Teweldebrhan, F. Miao, Superior thermal conductivity of single-layer graphene, Nano. Lett. 8(3) (2008) 902–917.

[20] K. Novoselov, A.K. Geim, S. Morozov, D. Jiang, M. Katsnelson, I. Grigorieva, Two-dimensional gas of massless Dirac fermions in graphene, Nature 438(7065), 197–200 (2005).

[21] Y. Zhu, S. Murali, W. Cai, X. Li, J.W. Suk, J.R Potts, Graphene and graphene oxide: synthesis, properties, and applications, Adv. Mater. 22(35) (2010) 3906–3924.

[22] C. Lee, X.D. Wei, J.W. Kysar, J. Hone, Measurement of the elastic properties and intrinsic strength of monolayer graphene, Sci. 321(5887) (2008) 385–388.

[23] F. Yavari, M. Rafiee, J. Rafiee, Z.Z. Yu, N. Koratkar, Dramatic increase in fatigue life in hierarchical graphene composites, ACS Appl. Mater. Interf. 2(10) (2010) 2738–2743.

[24] E. Mannov, H. Schmutzler, S. Chandrasekaran, C. Viets, S. Buschhorn, F. Tölle, Improvement of compressive strength after impact in fibre reinforced polymer composites by matrix modification with thermally reduced graphene oxide, Compos. Sci. Technol. 87 (2013) 36–41.

[25] D.G. Papageorgiou, I.A. Kinloch, R.J. Young, Hybrid multifunctional graphene/glass-fibre polypropylene composites, Compos. Sci. Technol. 137 (2016) 44–51.

[26] A.K. Pathak, M. Borah, A. Gupta, T. Yokozeki, S.R. Dhakate, Improved mechanical properties of carbon fiber/graphene oxide-epoxy hybrid composites, Compos. Sci. Technol. 135 (2016) 28–38.

[27] ASTM D7136. Standard Test Method for Measuring the Damage Resistance of a Fiber-Reinforced Polymer Matrix Composite to a Drop-Weight Impact Event.

[28] A. Elmarakbi, P. Karagiannidis, A. Ciappa, F. Innocente, F. Galise, B. Martorana, F. Bertocchi, F. Cristiano, A. Villaro, J. Gómez, 3-phase hierarchical graphene-based epoxy nanocomposite laminates for automotive applications, Mater. Sci. Tech. 35(10) (2019) 2169-2177.

[29] R. Ciardiello, B. Martorana, V.G. Lambertini, V. Brunella, Iron-based reversible adhesives: Effect of particles size on mechanical properties, Proc. Inst. Mech. Eng. C. 232(8) (2018) 1446–1455

[30] R. Ciardiello, A. Tridello, V. Brunella, B. Martorana, D.S. Paolino, G. Belingardi, Impact response of adhesive reversible joints made of thermoplastic nanomodified adhesive, J. Adhes. 94(12) (2018) 1051-1066.

[31] G. Belingardi, R. Vadori, Influence of the laminate thickness in low velocity impact behavior of composite material plate, Compos. Struct. 61 (2003) 27–38.

[32] G. Belingardi, M.P. Cavatorta, D.S. Paolino, On the rate of growth and extent of the steady damage accumulation phase in repeated impact tests, Compos. Sci. Technol. 69 (2009) 1693–1698.

[33] F. Wang, L. T. Drzal, Y. Qin, Z. Huang, Enhancement of fracture toughness, mechanical and thermal properties of rubber/epoxy composites by incorporation of graphene nanoplatelets. Composites: Part A 87 (2016) 10–22

[34] J. Ervina, M. Mariattia, S. Hamdan, Effect of Filler Loading on the Tensile Properties of Multi-walled Carbon Nanotube and Graphene Nanopowder filled Epoxy Composites. Procedia Chemistry 19 (2016) 897 – 905.

[35] F. Wang, L.T. Drzal, Y. Qin, Z. Huang, Size effect of graphene nanoplatelets on the morphology and mechanical behavior of glass fiber/epoxy composites, J. Mater. Sci. 51 (2016) 3337–3348.

[36] R. Palazzetti, A. Zucchelli, I. Trendafilova, The self-reinforcing effect of Nylon 6,6 nano-fibres on CFRP laminates subjected to low velocity impact. Composite Structures 106 (2013) 661–671.

[37] E. G. Koricho , A. Khomenko, M. Haq, L. T. Drzal, G. Belingardi, B. Martorana, Effect of hybrid (micro- and nano-) fillers on impact response of GFRP composite. Composite Structures 134 (2015) 789–798.

[38] F. Aymerich, A. Dalla Via, M. Quaresimin, Energy absorption capability of nanomodified glass/epoxy laminates. Procedia Engineering 10 (2011) 780–785.

[39] S.I. Abdullah, M.N.M. Ansari, Mechanical properties of graphene oxide (GO)/epoxy composites, HBRC J. 11 (2015) 151-156.